# P-Selectin Glycoprotein Ligand-1 Deficiency Is Protective Against Obesity-Related Insulin Resistance

**Chikage Sato,[1,2] Kenichi Shikata,[1,3] Daisho Hirota,[1] Motofumi Sasaki,[1] Shingo Nishishita,[1] Satoshi Miyamoto,[1] Ryo Kodera,[1] Daisuke Ogawa,[1,2] Atsuhito Tone,[1] Hitomi Usui Kataoka,[1] Jun Wada,[1] Nobuo Kajitani,[1] and Hirofumi Makino[1]**

**OBJECTIVE—**An inflammatory process is involved in the mechanism of obesity-related insulin resistance. Recent studies indicate that monocyte chemoattractant protein-1 (MCP-1) is a major chemokine that promotes monocyte infiltration into adipose tissues; however, the adhesion pathway in adipose tissues remains unclear. We aimed to clarify the adhesion molecules that mediate monocyte infiltration into adipose tissue.

**RESEARCH DESIGN AND METHODS—**We used a DNA microarray to compare the gene expression profiles in epididymal white adipose tissues (eWAT) between *db/db* mice and C57/BL6 mice each fed a high-fat diet (HFD) or a low-fat diet (LFD). We investigated the change of insulin resistance and inflammation in eWAT in P-selectin glycoprotein ligand-1 (PSGL-1) homozygous knockout (PSGL-1$^{-/-}$) mice compared with wild-type (WT) mice fed HFD.

**RESULTS—**DNA microarray analysis revealed that PSGL-1, a major ligand for selectins, is upregulated in eWAT from both *db/db* mice and WT mice fed HFD. Quantitative real-time RT-PCR and immunohistochemistry showed that PSGL-1 is expressed on both endothelial cells and macrophages in eWAT of obese mice. PSGL-1$^{-/-}$ mice fed HFD showed a remarkable reduction of macrophage accumulation and expression of proinflammatory genes, including MCP-1 in eWAT. Moreover, adipocyte hypertrophy, insulin resistance, lipid metabolism, and hepatic fatty change were improved in PSGL-1$^{-/-}$ mice compared with WT mice fed HFD.

**CONCLUSIONS—**These results indicate that PSGL-1 is a crucial adhesion molecule for the recruitment of monocytes into adipose tissues in obese mice, making it a candidate for a novel therapeutic target for the prevention of obesity-related insulin resistance. ***Diabetes*** **60:189–199, 2011**

Obesity is correlated closely with chronic low-grade inflammation in adipose tissues and insulin resistance, which causes systemic metabolic disorders (1). Accumulation of macrophages in adipose tissue is positively correlated with body weight and insulin resistance in both humans and rodents (2,3). Adipose tissue macrophages (ATMs) secrete a variety of proinflammatory cytokines and chemokines, including tumor necrosis factor (TNF)-α (4), interleukin (IL)-6, and monocyte chemoattractant protein (MCP)-1 (5), which enhance insulin resistance. ATM accumulation and insulin resistance are ameliorated in MCP-1–deficient mice (6) and C-C chemokine receptor 2 (CCR2)-deficient mice (7) fed a high-fat diet (HFD). Conversely, overexpression of MCP-1 resulted in increased numbers of ATMs along with the development of insulin resistance (6,8). These findings indicate that ATMs enhance obesity-related insulin resistance.

Monocyte infiltration into inflamed tissues is promoted by chemokines and adhesion molecules that are expressed on endothelial cells and monocytes (9). Selectin molecules and those ligands mediate leukocytes rolling along the activated endothelium, which is the first step of leukocyte recruitment into inflamed tissues. The second step is monocyte adhesion on endothelial cells mediated by intercellular adhesion molecule-1 (ICAM-1) or vascular cell adhesion molecule-1 (VCAM-1). Earlier, we reported that an inflammatory process is involved in the pathogenesis of diabetic nephropathy and that ICAM-1 deficiency is protective against the development of renal injury in diabetic mice without change of blood glucose (10–13). Several studies in humans have shown that serum levels of soluble ICAM-1 are elevated in obesity and positively correlate with central adiposity (14,15) and insulin resistance (16). Other studies have shown that serum levels of soluble E-selectin are associated with BMI or insulin resistance (17,18).

The predominant adhesion pathway of monocyte infiltration into adipose tissue is unclear. To clarify the adhesion molecules that promote monocyte infiltration into obese adipose tissue, we screened the gene expression profiles of adhesion molecules in adipose tissues from two different types of obese model mice and evaluated the functions of the candidate gene using gene knockout mice.

From the [1]Department of Medicine and Clinical Science, Okayama University Graduate School of Medicine, Dentistry and Pharmaceutical Sciences, Okayama, Japan; the [2]Department of Diabetic Nephropathy, Okayama University Graduate School of Medicine, Dentistry and Pharmaceutical Sciences, Okayama, Japan; and the [3]Center for Innovative Clinical Medicine, Okayama University Hospital, Okayama, Japan.

Corresponding author: Kenichi Shikata, shikata@md.okayama-u.ac.jp.

Received 26 December 2009 and accepted 7 October 2010. Published ahead of print at http://diabetes.diabetesjournals.org on 22 October 2010. DOI: 10.2337/db09-1894.



## RESEARCH DESIGN AND METHODS

**Animals and animal care.** Six-week-old C57/BL6 (BL6) mice were purchased from CLEA Japan (Tokyo, Japan). The *db/db* mice (C57BL/KsJ-*db/db*) and P-selectin glycoprotein ligand-1 (PSGL-1) homozygous knockout (PSGL-1$^{-/-}$) mice on the C57/BL6J background (19,20) were purchased as 6-week-old animals from The Jackson Laboratory (Bar Harbor, ME). All mice used in this study were males and were maintained under a 12-h light/12-h dark cycle with access to food and tap water ad libitum. The animal care and all procedures were done according to the Guidelines for Animal Experimentation at Okayama University Medical School, the Japanese Government Animal Protection and Management Law (number 105), and the Japanese Government Notification on Feeding and Safekeeping of Animals (number 6).

**Experimental protocol**

***Protocol 1.*** The *db/db* mice and the WT (C57/BL6) mice were fed a normal diet (Oriental Yeast, Osaka, Japan). All mice were killed at 8 weeks old, and

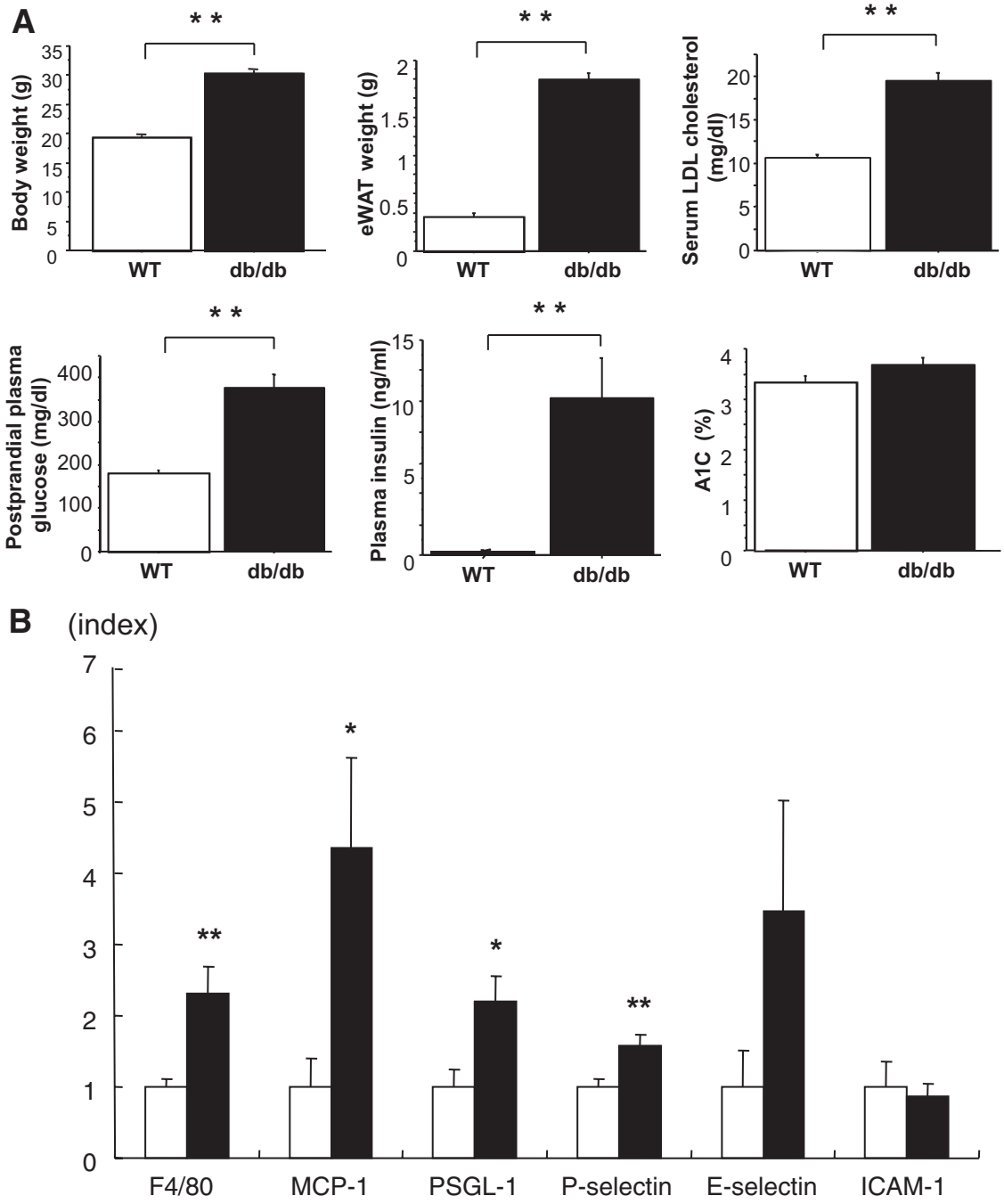


**FIG. 1. *A*: Metabolic characteristics of *db/db* and WT mice. Metabolic parameters of 8-week-old WT mice (□) and *db/db* mice (■) are shown. *B*: Gene expression in epididymal fat from 8-week-old WT mice (□) and *db/db* mice (■) analyzed by quantitative real-time RT-PCR. Data are means ± SE. *$P < 0.05$, **$P < 0.005$ vs. WT. $n = 10$ for each group.**

epididymal white adipose tissue (eWAT) was harvested, weighed, and fixed in 10% (vol/vol) formalin. The remaining tissue was stored at −80°C.

***Protocol 2.*** BL6 mice were fed HFD consisting of 60% kcal fat or a low-fat diet (LFD) consisting of 10% kcal fat (D12492 and D12450B, respectively; Research Diets, New Brunswick, NJ) from 7 to 19 weeks old. Intraperitoneal glucose and insulin tolerance tests were done at 15 or 16 weeks old. All mice were killed at 19 weeks old.

***Protocol 3.*** PSGL-$1^{-/-}$ and PSGL-$1^{+/+}$ (WT; C57/BL6) mice were fed HFD from 7 to 17 weeks old. Intraperitoneal glucose and insulin tolerance tests were done at 15 or 16 weeks old. All mice with <40 g body weight were killed at 17 weeks old. PSGL-$1^{-/-}$ mice were healthy and showed delayed neutrophil recruitment and moderate neutrophilia.

**Analysis of metabolic parameters.** Body weight and food intake were monitored weekly. For the glucose tolerance test, the mice were injected with glucose (1.2 g/kg body mass i.p.) after fasting for 12–16 h. For the insulin tolerance test, mice allowed access to food ad libitum were injected with human regular insulin (0.7 units/kg body mass i.p., Eli Lilly, Indianapolis, IN). We measured the concentration of glucose with a blood glucose meter (Glutest Pro; Sanwa Kagaku Kenkyusho, Nagoya, Japan), plasma insulin and leptin with an assay kit (Morinaga Institute of Biological Science, Kanagawa, Japan), and plasma adiponectin with an ELISA kit (Otsuka Pharmaceutical, Tokyo, Japan).

**RNA preparation from eWAT and liver.** Total RNA was extracted from each specimen of eWAT and liver using the RNeasy Lipid Tissue Mini Kit or RNeasy Plus Mini Kit following the instructions provided by the manufacturer (Qiagen, Valencia, CA).

**DNA microarray analysis.** We used five RNA samples from each group (*db/db* versus WT mice and BL6 mice fed HFD versus LFD) for DNA microarray analysis. Preparation of cRNA and hybridization of probe arrays (Mouse Genome 430 2.0) were performed according to the manufacturer's

TABLE 1
DNA microarray analysis

| | |
|---|---|
| Fibulin 2 | Selectin, lymphocyte |
| CD97 antigen | Integrin alpha x |
| Parvin, gamma | C-type lectin domain family 7, member a |
| C-type lectin domain family 4, member e | Metastasis suppressor 1 |
| A disintegrin and metallopeptidase domain 8 | Procollagen, type iii, alpha 1 |
| Integrin alpha m | Scavenger receptor class b, member 2 |
| Killer cell lectin-like receptor, subfamily a, member 2 | Protein tyrosine phosphatase, non-receptor type substrate 1 |
| Procollagen, type I, alpha 1 | Proline-serine-threonine phosphatase-interacting protein 1 |
| *Selectin, platelet (p-selectin) ligand* | Colony-stimulating factor 3 receptor (granulocyte) |
| Integrin alpha 7 | CD36 antigen |
| Expressed sequence c79673 | Ninjurin 1 |
| Procollagen, type v, alpha 3 | Vav 1 oncogene |
| Plakophilin 2 | Glycoprotein (transmembrane) nmb |
| Elastin microfibril interfacer 2 | CD22 antigen |
| Cell adhesion molecule with homology to l1cam | Riken cdna c030017f07 gene |
| Integrin beta 2 | Secreted phosphoprotein 1 |
| Milk fat globule-EGF factor 8 protein | Protocadherin 19 |
| Pleckstrin homology, sec7 and coiled-coil domains, binding protein | Procollagen, type viii, alpha 1 |
| CD44 antigen | Integrin beta 1 binding protein 1 |
| Calsyntenin 2 | Parvin, beta |
| Carboxypeptidase x 1 (m14 family) | Leupaxin |
| A disintegrin and metallopeptidase domain 23 | Neuropilin 2 |
| Oxidized low density lipoprotein (lectin-like) receptor 1 | Complement component 1, q subcomponent, receptor 1 |
| Procollagen, type v, alpha 2 | |

Gene ontology of cell adhesion category of more than twice upregulated genes *db/db* versus wild-type mice is shown (total, 47 genes).

instructions (Affymetrix, Santa Clara, CA). These arrays contain probe sets for >45,000 transcripts. The criteria for selecting genes were as follows: *1*) genes whose flags were "present" and *2*) ratio of expression level of >2.0-fold increase in *db/db* compared with WT mice or in BL6 mice fed HFD compared with LFD. Gene Ontology Biological Process classification of the >2.0-fold upregulated genes from each group was done with the DAVID Bioinformatics Database functional-annotation tools (http://niaid.abcc.ncifcrf.gov) (21).

**Quantitative real-time RT-PCR analysis for eWAT and liver.** The mRNA expression of each gene was measured by quantitative real-time RT-PCR as described previously (22). The amounts of PCR products were normalized with a housekeeping gene (β-actin or GAPDH) to calculate the relative expression ratios. Each experiment was done in triplicate. The primers were as follows: MCP-1: 5′-AAGCTGTAGTTTTTGTCACC-3′ (forward), 5′-GGGCA GATGCAGTTTTAA-3′ (reverse); PSGL-1 (Selpl): 5′-TTGTGCTGCTGAC CATCT-3′ (forward), 5′-TCCTCAAAATCGTCATCC-3′ (reverse); P-selectin (Selp): 5′-CAGTGGCTTCTACAACAGGC-3′ (forward), 5′-T GGGTCATATG CAGCGTTA-3′ (reverse); E-selectin (Sele): 5′-CATGGCTCAGCTCAACTT-3′ (forward), 5′-GCAGCTCATGTTCATCTT-3′ (reverse); CD68: 5′-GCGGTG GAATACAATGTG-3′ (forward), 5′-AGAGAGAGCAGGTCAAGGT-3′ (reverse); β-actin: 5′-CCTGTATGCCTCTGGTCGTA-3′ (forward), 5′-CCATCTCCTGCTC GAAGTCT-3′ (reverse).

These primers were purchased from Nihon Gene Research Labs (Sendai, Japan). ICAM-1 (GenBank accession code X52264, cat. no. 4651782) and NOS2 (iNOS) (GenBank accession code NM_010927, cat. no. 5026474) were in the Light Cycler-Primer Set (Roche Diagnostics, Rotkreuz, Switzerland). F4/80 (Mm01236959_m1), CD11c (Mm00498698_m1), IL-10 (Mm01288386_m1), IL-6 (Mm0046190_m1), LPL (Mm00434770_m1), leptin (Mm00434759_m1), fatty acid synthase (FAS) (Mm00662319_m1), sterol regulatory element binding protein-1c (SREBP-1c) (Mm0113844_m1), acetyl-CoA carboxylase-1 (ACC-1) (Mm01304289_m1), and peroxisome proliferator–activated receptor-α (PPAR-α) (Mm00627559_m1) were TaqMan gene expression assays (Applied Biosystems, Tokyo, Japan).

**Isolation of adipocytes and stromal-vascular fractions.** Stromal vascular fraction (SVF) cells and peripheral blood mononuclear cells (PBMCs) were isolated from *db/db* mice or BL6 mice at 10 weeks of age. SVF cells were isolated as described (23,24). PBMCs were separated by density gradient centrifugation using a Lymphocyte Separation Medium (MP Biomedicals, Solon, OH). Cells in the SVF and PBMCs were analyzed by flow cytometry.

**Flow cytometry analysis.** SVF cells or PBMCs were suspended in Pharmingen stain buffer (BD Biosciences, San Jose, CA) and incubated for 10 min with Fc-block and then with primary antibodies or the matching control isotypes for 30 min at 4°C. Then, the pellets were incubated with RBC Lysis Buffer (eBioscience, San Diego, CA) for 5 min and rinsed twice with Pharmingen stain buffer. After incubation with 7-amino-actinomycin D (BD Biosciences), the cells were analyzed using a FACS Calibur (BD Biosciences). Data analysis was performed using CELL Quest (BD Biosciences).

**In vivo Akt phosphorylation.** WT mice and PSGL-1$^{-/-}$ mice fed HFD were starved for 14 h, anesthetized with pentobarbital, and injected with 5 units of regular human insulin into the inferior vena cava. Five minutes later, the livers, eWAT, and hindlimb muscle were excised and stored at −80°C until use. Tissue samples were homogenized in RIPA Lysis buffer (Santa Cruz Biotechnology, Santa Cruz, CA) at 4°C. After centrifugation at 13,000 rpm for 30 min at 4°C, supernatant was collected. Total protein concentration was determined by using the DC-protein determination system (Bio-Rad Laboratories) and an equivalent amount of protein (40–60 μg). Samples were resolved by SDS-PAGE and transferred to a nitrocellulose membrane with iBlot Dry Blotting System (Invitrogen). The membranes were blocked with 5% nonfat dry milk in 1× Tris-buffered saline containing 0.1% Tween-20 for 1 h and incubated overnight with anti–phospho-Akt (Ser473) antibody and anti-Akt antibody (Cell Signaling Technology, Danvers, MA) at 4°C. After incubation with horseradish peroxidase–labeled secondary antibodies for 1 h, signals were detected with an enhanced chemiluminescence system (Amersham). Membranes were exposed in an Image system LAS-3000 (FujiFilm) and analyzed by using Image J software.

**Light microscopy and morphometric analysis of adipocyte area.** eWAT was isolated from mice, fixed in 10% formalin, and embedded in paraffin. Paraffin sections (4 μm thick) were deparaffinized and rehydrated and then stained with periodical acid Schiff stain. The adipocyte area was traced manually and analyzed with Lumina Vision OL V2.4.4 software (Mitani, Tokyo, Japan). The area was measured in six high-power fields from each of five mice.

**Immunohistochemical staining.** Immunoperoxidase and immunofluorescent staining were done as described (11,12,25). Paraffin sections were deparaffinized and rehydrated before antigen unmasking by boiling in R-Buffer U at a dilution of 1:10 (PickCell Laboratories, Amsterdam, the Netherlands) for 10 min.

We used immunoperoxidase staining for macrophage and PSGL-1 in eWAT of *db/db* mice and WT mice on normal food. Rat anti-mouse monocyte/macrophage (Mac-3) monoclonal antibody (mAb) at a dilution of 1:50 (Santa Cruz Biotechnology) and rat anti-mouse PSGL-1 (CD162) mAb at a dilution of 1:50 (Fitzgerald Industries International, Concord, MA) were applied to the sections as the primary reaction, followed by a second reaction with biotin-labeled donkey anti-rat IgG antibody (Jackson Immunoresearch Laboratories, West Grove, PA) at a dilution of 1:50. The avidin-biotin coupling reaction was done with the Vectastain Elite kit (Vector Laboratories, Burlingame, CA).

We used double immunofluorescence staining to clarify the expression and localization of PSGL-1, leukocyte/macrophage, and endothelial cells in eWAT of *db/db* mice. PSGL-1 mAb followed by Alexa Fluor 488 donkey anti-rat IgG (A-21208; Molecular Probes, Eugene, OR) and goat anti-mouse leukocyte/macrophage (CD45) mAb (sc-1121; Santa Cruz Biotechnology) followed by

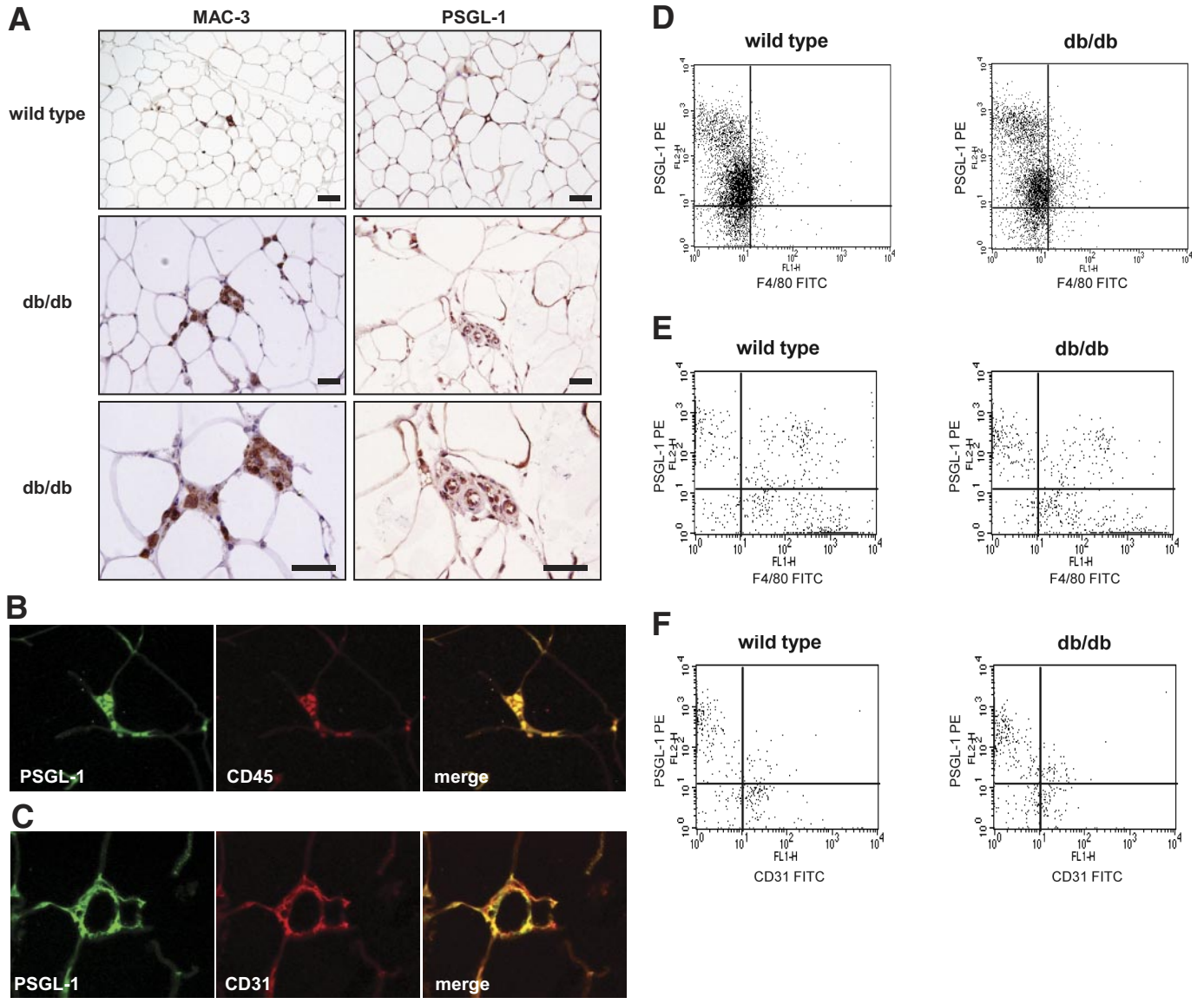


**FIG. 2.** ***A*: Immunohistochemical localization of PSGL-1, macrophages, and endothelial cells in adipose tissue. Epididymal fat pads from 8-week-old *db/db* mice and WT mice were stained with anti–MAC-3 (*left-hand panels*) and anti–PSGL-1 antibodies (*right-hand panels*). Macrophages and PSGL-1 expressed around the small vessels in the interstitium of adipose tissue in *db/db* mice are shown. The scale bars represent 50 μm. *B*: Double immunofluorescence staining of adipose tissue from *db/db* mice with the antibodies against PSGL-1 (*green*) and leukocyte (CD45, *red*). PSGL-1 and CD45 were stained in the interstitium of adipose tissue and are colocalized in the merged picture. *C*: Double immunofluorescence staining of adipose tissue from *db/db* mice with the antibodies against PSGL-1 (*green*) and endothelial cell (CD31, *red*). PSGL-1 and CD31 were stained along small vessels of adipose tissue and are colocalized in the merged picture. *D–F*: The expression of PSGL-1 on cells in WT mice and *db/db* mice was analyzed using flow cytometry. *D*: The expression of PSGL-1 in PBMCs. *E*: The expression of PSGL-1 in F4/80$^+$ macrophages in the SVF from adipose tissue. *F*: The expression of PSGL-1 in CD31$^+$ endothelial cells in the SVF from adipose tissue. (A high-quality digital representation of this figure is available in the online issue.)**

Alexa Fluor 546 rabbit anti-goat IgG (A-21085; Molecular Probes) were applied to the sections. Similarly, PSGL-1 mAb followed by Alexa Fluor 488 donkey anti-rat IgG and goat anti-mouse endothelial cell (PECAM-1/CD31) mAb (sc-1506; Santa Cruz Biotechnology) followed by Alexa Fluor 546 rabbit anti-goat IgG were applied to the sections.

**Measurement of hepatic triglyceride content.** Measurement of the hepatic triglyceride content in WT mice and PSGL-1$^{-/-}$ mice fed HFD was done by the Folch technique (26) at Skylight Biotech (Akita, Japan), and the triglyceride concentration was measured with Cholestest TG (Sekisui Medical, Tokyo, Japan). The tissue triglyceride concentrations were corrected for liver weight.

**Statistical analysis.** All data are expressed as mean ± SE and were analyzed by the Mann-Whitney *U* test with the level of statistical significance set at $P < 0.05$.

## RESULTS

**Analysis of eWAT from *db/db* mice.** The *db/db* mice showed significantly increased body weight, weight of eWAT, levels of serum LDL cholesterol, postprandial plasma glucose, and plasma insulin compared with WT mice, but A1C was not different between the two groups (Fig. 1*A*).

DNA microarray analysis detected 1,080 genes that were more than twofold upregulated in *db/db* mice compared with WT mice. Gene ontology analysis indicated that 47 cell adhesion-related genes, including L-selectin (2.0-fold change, *db/db* versus wild-type) and PSGL-1 (2.0-fold change, *db/db* versus wild-type) were upregulated in *db/db* mice compared with WT mice (supplementary Fig. 1, available in an online-only appendix at http://diabetes.diabetesjournals.org/cgi/content/full/db09-1894/DC1; Table 1).

We focused on PSGL-1 because it is expressed on both

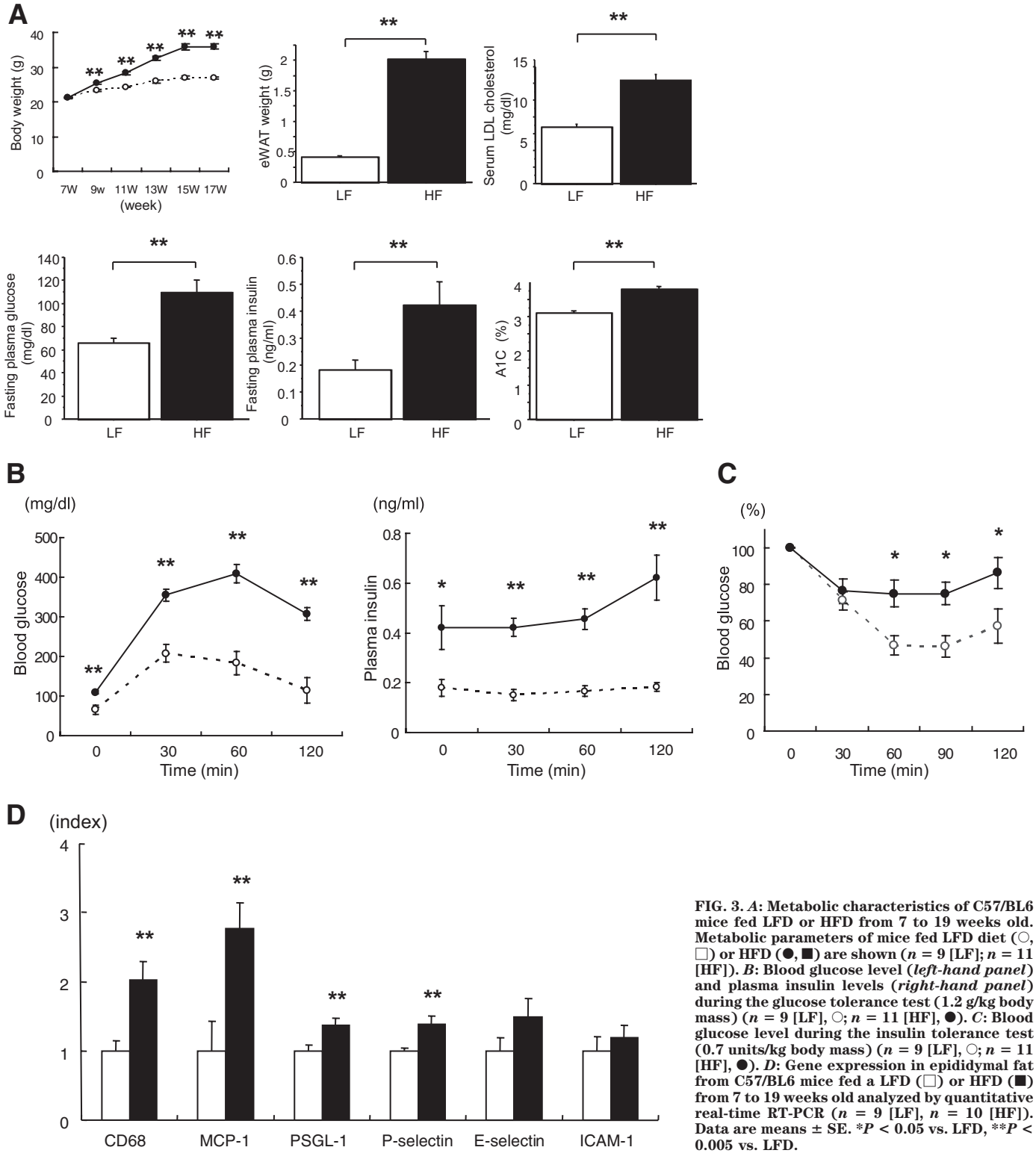


**FIG. 3. *A*: Metabolic characteristics of C57/BL6 mice fed LFD or HFD from 7 to 19 weeks old. Metabolic parameters of mice fed LFD diet (○, □) or HFD (●, ■) are shown ($n$ = 9 [LF]; $n$ = 11 [HF]). *B*: Blood glucose level (*left-hand panel*) and plasma insulin levels (*right-hand panel*) during the glucose tolerance test (1.2 g/kg body mass) ($n$ = 9 [LF], ○; $n$ = 11 [HF], ●). *C*: Blood glucose level during the insulin tolerance test (0.7 units/kg body mass) ($n$ = 9 [LF], ○; $n$ = 11 [HF], ●). *D*: Gene expression in epididymal fat from C57/BL6 mice fed a LFD (□) or HFD (■) from 7 to 19 weeks old analyzed by quantitative real-time RT-PCR ($n$ = 9 [LF], $n$ = 10 [HF]). Data are means ± SE. *$P$ < 0.05 vs. LFD, **$P$ < 0.005 vs. LFD.**

leukocytes and endothelium and has a wide range of binding capacity to all three types of selectin (27–29). Real-time RT-PCR demonstrated that PSGL-1 mRNA expression was significantly higher in eWAT of *db*/*db* mice compared with that in WT mice. The transcriptional levels of other proinflammatory genes, including F4/80, MCP-1, and P-selectin mRNA, were also increased significantly in *db*/*db* mice (Fig. 1*B*), whereas the mRNA expression of other adhesion molecule genes, such as E-selectin and ICAM-1, in *db*/*db* mice was not different from that in WT mice.

Immunoperoxidase staining was used for MAC-3, a macrophage marker, and PSGL-1 in eWAT from *db*/*db* mice and WT mice fed normal diet. The expression of macrophage and PSGL-1 increased around the small vessels in the interstitium of eWAT in *db*/*db* mice (Fig. 2*A*). Furthermore, to estimate the distribution of PSGL-1, macrophage, and endothelial cells in eWAT, we used double

TABLE 2
DNA microarray analysis

| | |
|---|---|
| Connective tissue growth factor | CD44 antigen |
| TNF receptor superfamily, member 12a | Procollagen, type vi, alpha 3 |
| Thrombospondin 1 | Carboxypeptidase x 1 (m14 family) |
| Cysteine rich protein 61 | Cartilage acidic protein 1 |
| rho GTPase activating protein 6 | Integrin alpha x |
| Procollagen, type VI, alpha 2 | C-type lectin domain family 7, member a |
| Riken cdna 2700007f12 gene | Vav 3 oncogene |
| A disintegrin and metallopeptidase domain 8 | Neural precursor cell expressed, developmentally downregulated gene 9 |
| CD9 antigen | Discoidin, cub and lccl domain containing 2 |
| Poliovirus receptor | Procollagen, type vi, alpha 1 |
| Filamin binding lim protein 1 | Periostin, osteoblast specific factor |
| A disintegrin and metallopeptidase domain 12 (meltrin alpha) | Protein tyrosine phosphatase, non-receptor type substrate 1 |
| Calsyntenin 3 | Proline-serine-threonine phosphatase-interacting protein 1 |
| Poliovirus receptor-related 3 | Tenascin c |
| Integrin alpha m | Vav 1 oncogene |
| *Selectin, platelet (p-selectin) ligand* | Glycoprotein (transmembrane) nmb |
| Procollagen, type I, alpha 1 | Activated leukocyte cell adhesion molecule |
| Expressed sequence c79673 | Secreted phosphoprotein 1 |
| Immunoglobulin superfamily, member 4a | Procollagen, type viii, alpha 1 |
| Integrin beta 2 | Leupaxin |
| Pleckstrin homology, sec7 and coiled-coil domains, binding protein | |

Gene ontology of cell adhesion category of more than twice upregulated genes HFD versus LFD is shown (total, 41 genes).

immunofluorescence staining in eWAT from *db/db* mice. PSGL-1 (*green*) and leukocyte/macrophage (CD45, *red*) were detected in the interstitium of eWAT. They were mostly coexpressed in a merged picture (Fig. 2*B*). In addition, PSGL-1 (*green*) and endothelial cells (CD31, *red*) were mostly detected in the interstitium of eWAT and mostly coexpressed in a merged picture (Fig. 2*C*).

We examined PBMCs from WT mice or *db/db* mice. $F4/80^+PSGL\text{-}1^+$ cells were similarly contained (WT mice $82.3 \pm 1.2\%$ versus *db/db* mice $84.6 \pm 2.5\%$ of $F4/80^+$ cells, $P = 0.827$) between the two groups by flow cytometry analysis. We isolated SVF cells from epididymal fat pads excised from WT mice or *db/db* mice fed a normal diet and analyzed cells by flow cytometry. $F4/80^+PSGL\text{-}1^+$ cells were not different (WT mice $23.2 \pm 2.2\%$ versus *db/db* mice $34.3 \pm 4.3\%$ of $F4/80^+$ cells, $P = 0.149$) between WT mice and *db/db* mice. $CD31^+PSGL\text{-}1^+$ cells significantly increased (WT mice $36.6 \pm 2.5\%$ versus *db/db* mice $53.9 \pm 3.5\%$ of $CD31^+$ cells, $P = 0.021$) in *db/db* mice compared with WT mice (Fig. 2*D–F*). These results indicate that $CD31^+PSGL\text{-}1^+$ cells were increased in adipose tissue of *db/db* mice.

**Upregulation of PSGL-1 expression in BL6 mice fed HFD.** We next examined eWAT in BL6 mice fed LFD or HFD to determine whether PSGL-1 expression increased in HFD-induced obese mice. BL6 mice fed HFD showed significantly increased body weight, weight of eWAT, serum LDL cholesterol, fasting plasma glucose, plasma insulin, and A1C compared with BL6 mice fed LFD (Fig. 3*A*). Plasma glucose and insulin levels during a glucose tolerance test were markedly higher in BL6 mice fed HFD compared with mice fed LFD (Fig. 3*B*). Similarly, BL6 mice fed HFD showed impaired insulin sensitivity as measured by the insulin tolerance test (Fig. 3*C*).

DNA microarray profiling indicated that 572 genes were upregulated more than twofold in BL6 mice fed HFD compared with those fed LFD. Analysis by gene ontology categories showed that 41 cell adhesion–related genes, including *PSGL-1*, were upregulated in BL6 mice fed HFD (twofold change, HFD/LFD) (supplementary Fig. 2, Table 2). Quantitative real-time RT-PCR showed that transcriptional levels of CD68, MCP-1, PSGL-1, and P-selectin mRNA were increased significantly in BL6 mice fed HFD. E-selectin and ICAM-1 mRNA expression were not different between the two groups (Fig. 3*D*).

**PSGL-1 deficiency improved insulin sensitivity.** As described above, PSGL-1 was upregulated in eWAT of two different rodent models for obesity-related insulin resistance. We further examined the role of PSGL-1 in eWAT of diet-induced obese mice using PSGL-1–deficient ($PSGL\text{-}1^{-/-}$) mice. The $PSGL\text{-}1^{-/-}$ and $PSGL\text{-}1^{+/+}$ WT mice were fed HFD for 10 weeks.

Body weight, the weight of each adipose tissue per unit body weight, and food intake were not different between the two groups (Fig. 4*A*). There was no difference in fasting plasma glucose and A1C between the two groups, although fasting plasma insulin level was significantly lower in $PSGL\text{-}1^{-/-}$ mice than it was in WT mice fed HFD (Fig. 4*B*). These data indicated that PSGL-1 deficiency improved insulin resistance without a change of body weight or the amount of eWAT.

Intraperitoneal glucose and insulin tolerance tests were used to further confirm that PSGL-1 deficiency improves insulin sensitivity. Blood glucose levels during the glucose tolerance test were similar in the two groups, although plasma insulin levels were lower in $PSGL\text{-}1^{-/-}$ mice than those in WT mice fed HFD (Fig. 4*C*). The glucose-lowering effect of insulin was significantly greater in $PSGL\text{-}1^{-/-}$ mice than it was in WT mice, as measured by the insulin tolerance test (Fig. 4*D*). These data confirmed that insulin sensitivity was improved in $PSGL\text{-}1^{-/-}$ mice fed HFD.

To further investigate insulin sensitivity in $PSGL\text{-}1^{-/-}$ mice, we examined insulin-stimulated phosphorylation of Akt in liver and muscle. Akt phosphorylation in liver was not different between the two groups. However, Akt phosphorylation in muscle was significantly increased in $PSGL\text{-}1^{-/-}$ mice compared with WT mice fed HFD (Fig. 4*E*).

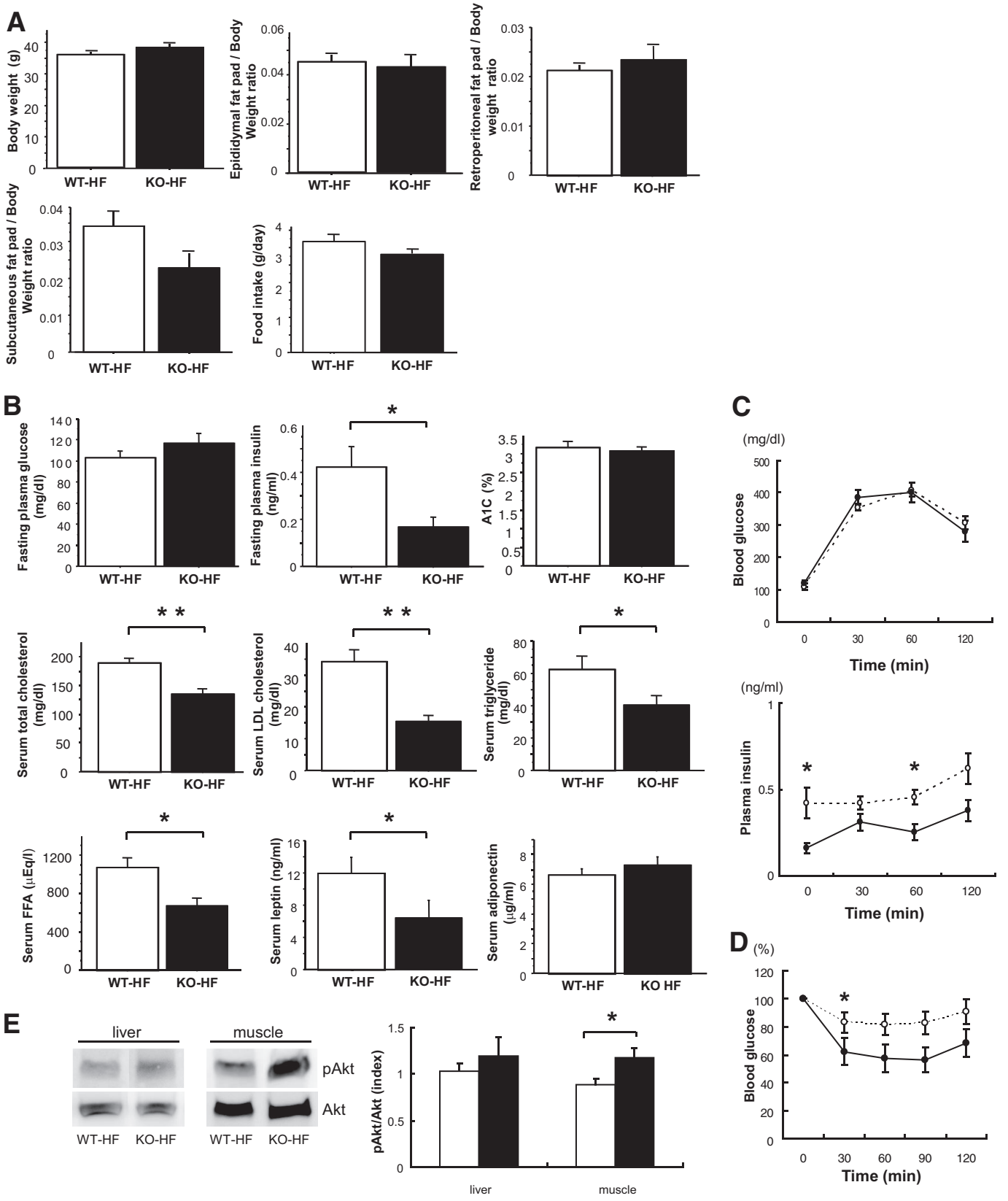


**FIG. 4.** ***A*****: Metabolic characteristics of WT mice and PSGL-1$^{-/-}$ (KO) mice fed HFD from 7 to 17 weeks old. Body composition and food intake in WT mice (□) and PSGL-1$^{-/-}$ mice (■) fed HFD ($n$ = 7 [WT-HF]; $n$ = 8 [KO-HF]) is shown.** ***B*****: Metabolic parameters of WT mice (□) and PSGL-1$^{-/-}$ mice (■) fed HFD ($n$ = 7 [WT-HF]; $n$ = 8 [KO-HF]).** ***C*****: Blood glucose level (*upper panel*) and plasma insulin levels (*lower panel*) during the glucose tolerance test (1.2 g/kg body mass) ($n$ = 9 [WT-HF], ○; $n$ = 8 [KO-HF], ●).** ***D*****: Blood glucose level during the insulin tolerance test (0.7 units/kg body mass) ($n$ = 9 [WT-HF], ○; $n$ = 8 [KO-HF], ●). Data are means ± SE. *$P$ < 0.05 vs. WT-HFD, **$P$ < 0.005 vs. WT-HFD.** ***E*****: Equal amounts of protein in total lysates of liver and muscle were immunoblotted with anti–phospho-Akt (pAkt) and anti-Akt antibodies. The relative ratio of Akt phosphorylation was calculated after normalization with the Akt signal ($n$ = 5 [WT-HF], □; $n$ = 5 [KO-HF], ■). Data are means ± SE. *$P$ < 0.05 vs. WT-HFD. FFA, free fatty acid.**

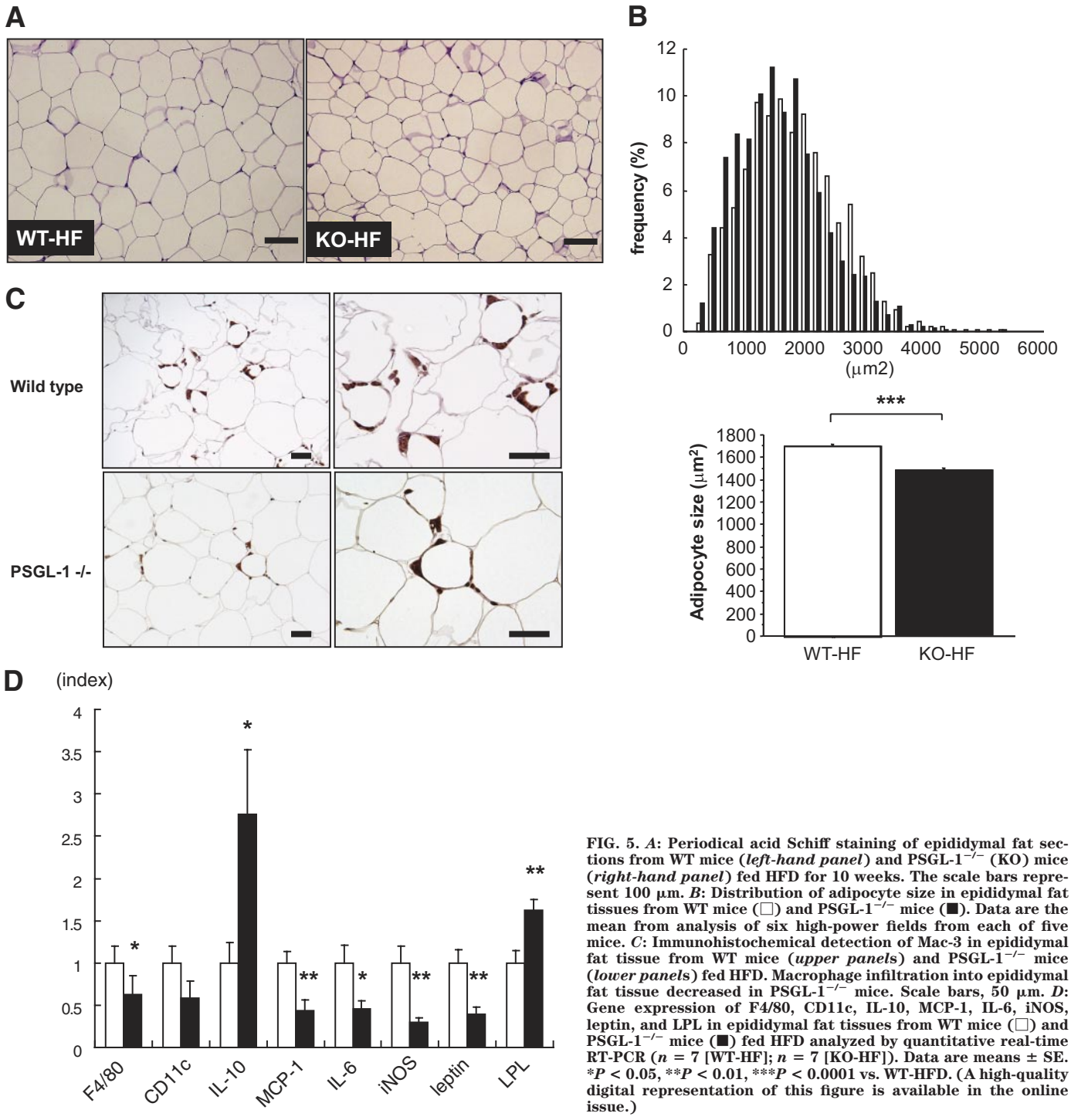


**FIG. 5.** ***A*: Periodical acid Schiff staining of epididymal fat sections from WT mice (*left-hand panel*) and PSGL-1$^{-/-}$ (KO) mice (*right-hand panel*) fed HFD for 10 weeks. The scale bars represent 100 μm. *B*: Distribution of adipocyte size in epididymal fat tissues from WT mice (□) and PSGL-1$^{-/-}$ mice (■). Data are the mean from analysis of six high-power fields from each of five mice. *C*: Immunohistochemical detection of Mac-3 in epididymal fat tissue from WT mice (*upper panels*) and PSGL-1$^{-/-}$ mice (*lower panels*) fed HFD. Macrophage infiltration into epididymal fat tissue decreased in PSGL-1$^{-/-}$ mice. Scale bars, 50 μm. *D*: Gene expression of F4/80, CD11c, IL-10, MCP-1, IL-6, iNOS, leptin, and LPL in epididymal fat tissues from WT mice (□) and PSGL-1$^{-/-}$ mice (■) fed HFD analyzed by quantitative real-time RT-PCR ($n$ = 7 [WT-HF]; $n$ = 7 [KO-HF]). Data are means ± SE. *$P$ < 0.05, **$P$ < 0.01, ***$P$ < 0.0001 vs. WT-HFD. (A high-quality digital representation of this figure is available in the online issue.)**

**PSGL-1 deficiency decreased macrophage infiltration and inflammation in obese adipose tissue.** Morphometric analysis demonstrated that adipocytes in eWAT were smaller in PSGL-1$^{-/-}$ mice than in WT mice fed HFD (Fig. 5*A* and *B*). Immunohistochemistry showed a decrease of MAC-3–positive cells in eWAT from PSGL-1$^{-/-}$ mice fed HFD (Fig. 5*C*). The mRNA expression of F4/80, MCP-1, IL-6, iNOS, and leptin was decreased in eWAT from PSGL-1$^{-/-}$ mice compared with that in WT mice fed HFD (Fig. 5*D*), although the levels of TNF-α and adiponectin mRNA were not statistically different between the two groups (data not shown). IL-10 mRNA levels were significantly increased, whereas CD11c mRNA levels tended to be decreased without significant difference in PSGL-1$^{-/-}$ mice fed HFD compared with WT mice fed HFD (Fig. 5*D*).

**PSGL-1 deficiency improved lipid metabolism and hepatic steatosis.** In this study, the weight of liver and the level of serum triglycerides were reduced significantly, and the hepatic triglyceride content tended to be decreased in PSGL-1$^{-/-}$ mice compared with WT mice fed HFD (Figs. 4*B* and 6*A*). The mRNA expression of CD68 was not different between the two groups. (Fig. 6*B*). A few lipid metabolism–related genes in liver were not different between the two groups as follows: FAS (WT-HF 9.37 ± 3.07 vs. KO-HF 5.37 ± 1.38, $P$ = 0.223), SREBP-1c (WT-HF 3.29 ± 0.48 vs. KO-HF 3.77 ± 0.64, $P$ = 0.685), ACC-1

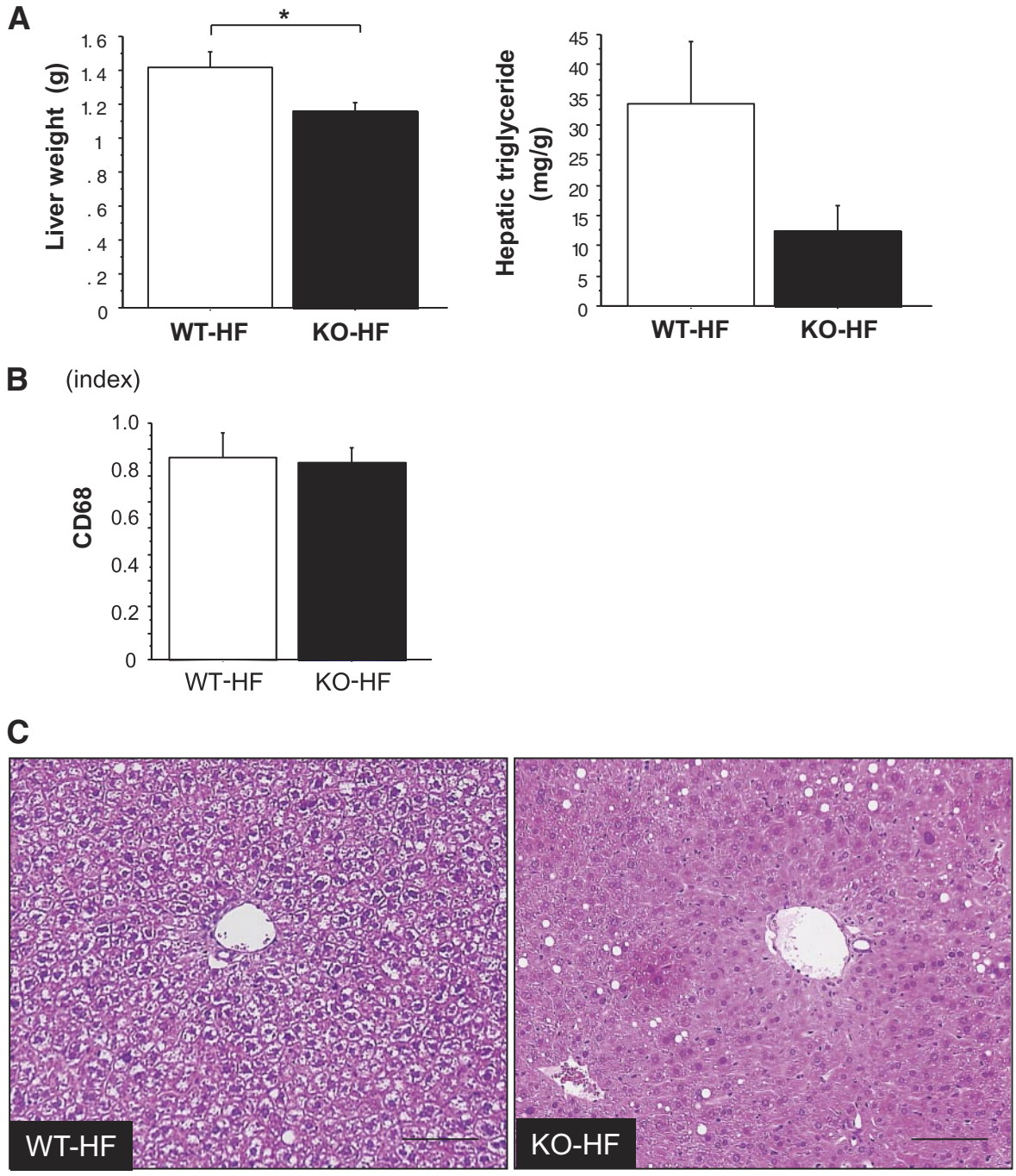


**FIG. 6.** *A*: Liver weight (*left*) and hepatic triglyceride (*right*) in WT mice (□) and PSGL-1$^{-/-}$ (KO) mice (■) fed HFD for 10 weeks ($n$ = 5 [WT-HF]; $n$ = 8 [KO-HF]). Data are means ± SE. *$P$ < 0.05 vs. WT-HFD. *B*: Gene expression of CD68 in liver from WT mice (□) and PSGL-1$^{-/-}$ mice (■) fed HFD diet analyzed by quantitative real-time RT-PCR ($n$ = 5 [WT-HF]; $n$ = 8 [KO-HF]). Data are means ± SE. *C*: Hematoxylin and eosin stain. Hepatic steatosis is prominent in the liver of WT mice fed HFD. The scale bars represent 100 μm. (A high-quality digital representation of this figure is available in the online issue.)

(WT-HF 20.25 ± 2.63 vs. KO-HF 19.59 ± 3.09, $P$ = 0.935), PPAR-α (WT-HF 24.45 ± 5.25 vs. KO-HF 22.93 ± 4.03, $P$ = 0.685), and LPL (WT-HF 1.17 ± 0.15 vs. KO-HF 1.95 ± 0.79, $P$ = 0.685). (The amounts of PCR products were normalized with a housekeeping gene [GAPDH] to calculate the relative expression ratios.) On the other hand, the mRNA expression of LPL in adipose tissue improved in PSGL-1$^{-/-}$ mice compared with WT mice fed HFD (Fig. 5*D*). Histologically, the liver of WT mice fed HFD showed massive hepatocyte ballooning around the central veins; however, the hepatic steatosis was improved in PSGL-1$^{-/-}$ mice fed HFD (Fig. 6*C*). Furthermore, the levels of serum total cholesterol, LDL, free fatty acids, and leptin were lower in PSGL-1$^{-/-}$ mice than in WT mice fed HFD (Fig. 4*B*), but aspartate aminotransferase and alanine aminotransferase were not different between the two groups (data not shown).

## DISCUSSION

To investigate the mechanism of monocytes/macrophages infiltration into adipose tissue, we used a DNA microarray

for obese adipose tissue in *db/db* mice or WT mice fed HFD. Both groups were in a state of intensive insulin resistance but were not diabetic. Expression of the adhesion molecule PSGL-1 was increased in obese adipose tissue from *db/db* mice and from WT mice fed HFD, as determined by DNA microarray analysis. In addition, an increase in PSGL-1 mRNA expression was observed with real-time RT-PCR and immunohistochemistry in obese adipose tissue. Furthermore, PSGL-1–deficient mice had reduced macrophage accumulation, insulin resistance, lipid metabolism, and steatohepatic change associated with obesity.

PSGL-1 was originally identified by expression cloning of a functional ligand for P-selectin (30). PSGL-1 is a mucin-like cell adhesion molecule expressed on the surface of leukocytes and endothelial cells and then involved in platelet-leukocyte and endothelium-leukocyte interactions. PSGL-1 mRNA was expressed in a variety of tissues, including bone marrow, brain, adipose tissue, heart, kidney, and liver. PSGL-1 is highly expressed in hematopoietic cells and in nonhematopoietic tissues, including adipose tissue and brain. The domain structure of PSGL-1 and amino acids are highly conserved between humans and rodents (31). PSGL-1 interacts with all three selectins: L-selectin (32), E-selectin (19,22), and P-selectin (29).

Earlier, it was reported that mice deficient in ICAM-1, or other leukocyte adhesion molecules, increased body weight and white fat pad weight (% of body weight) on normal food and on HFD. Mac-1 (αMβ2, CD11b/CD18) is a counter-receptor for ICAM-1, and Mac-1–deficient mice showed a similar obesity phenotype (33). A1C was not different in ICAM-1–deficient *db/db* mice, streptozotocin-induced ICAM-1–deficient mice, *db/db* mice (13), and streptozotocin-induced WT mice (12). Furthermore, the number of leukocytes in the adipose tissue of ICAM-1–deficient mice and Mac-1–deficient mice fed HFD were the same as in the WT mice fed HFD. Consequently, these adhesion receptors are not required for leukocyte migration into adipose tissue (34).

In this study, PSGL-1 expression on peripheral blood monocyte was not increased in *db/db* mice compared with WT mice. Moreover, PSGL-1 expression on ATMs was also similar between *db/db* mice and WT mice by flow cytometry analysis. On the other hand, $CD31^{+}PSGL\text{-}1^{+}$ cell content was significantly increased in the SVF of eWAT in *db/db* mice compared with WT mice. These results indicate that increased expression of PSGL-1 on endothelial cells in adipose tissue is involved in infiltration of macrophage and inflammation in adipose tissue of obese mice.

The accumulation of macrophages in adipose tissue is correlated with increased body weight and insulin resistance in both humans and rodents (2,3). MCP-1 contributed to macrophage infiltration into adipose tissue and insulin resistance in mice (6,8). Those reports indicated that the ATMs might play an important role in the development of insulin resistance. Moreover, there are recent reports that the polarization of macrophages is changed from M2 to M1 in obese inflamed adipose tissue (35). M1 macrophages are induced by proinflammatory mediators such as lipopolysaccharide and γ-interferon (IFN-γ) and produce proinflammatory cytokines TNF-α and IL-6. Instead, M2 macrophages generate high levels of anti-inflammatory cytokines IL-10 and IL-1. Our data showed that MCP-1, IL-6, and iNOS mRNA levels were reduced, and IL-10 mRNA, an M2 macrophage marker, was significantly increased in eWAT from $PSGL\text{-}1^{-/-}$ mice compared with WT mice fed HFD. Whereas CD11c mRNA as an M1 macrophage marker tended to be decreased in $PSGL\text{-}1^{-/-}$ mice compared with WT mice fed HFD. These results demonstrated that PSGL-1 deficiency reduced the number of ATMs and changed the phenotype of macrophages from M1 to M2 and then affected inhibition of inflammation in eWAT. Furthermore, PSGL-1 deficiency improved insulin signaling in the muscle, as evidenced by an increase in Akt phosphorylation in animals fed HFD. As a result, $PSGL\text{-}1^{-/-}$ mice fed HFD ameliorated systemic glucose tolerance and insulin sensitivity.

Several studies reported that blockade of PSGL-1 reduced inflammatory reactions. In the model of cold ischemia/reperfusion, hepatic endothelial neutrophil infiltration and hepatocyte injury were diminished, and the expression of TNF-α, IL-6, iNOS, IL-2, and IFN-γ mRNA was decreased in livers pretreated with recombinant PSGL-Ig (36). Other reports showed that blockade of PSGL-1 attenuated macrophage recruitment in intestinal mucosa and ameliorated ileitis in a mouse model of Crohn's disease (37,38).

In this study, serum triglyceride and hepatic steatosis improved in $PSGL\text{-}1^{-/-}$ mice fed HFD. The mRNA expression of LPL was improved in adipose tissue of $PSGL\text{-}1^{-/-}$ mice compared with WT mice fed HFD. These results might be explained if the amelioration of insulin resistance increased LPL in adipose tissue. Consequently, lipid metabolism, including serum free fatty acids, triglyceride, cholesterol, and hepatic triglycerides, might be improved in $PSGL\text{-}1^{-/-}$ mice compared with WT mice fed HFD.

We found that plasma leptin levels and leptin mRNA expression in eWAT were decreased in $PSGL\text{-}1^{-/-}$ mice fed HFD, despite no difference of body weight or weight of fat. The plasma leptin concentration is positively correlated with BMI and weight of body fat in humans (39). Obese individuals are generally in a state of leptin resistance, although the pathophysiology of leptin resistance has not been clarified. Our data suggested that improvement of leptin sensitivity resulted in lower levels of plasma leptin in $PSGL\text{-}1^{-/-}$ mice than that in WT mice fed HFD. However, further studies are needed to determine whether PSGL-1 deficiency improves leptin sensitivity in obese animals.

In conclusion, our results indicate that PSGL-1 is a crucial adhesion molecule for recruitment of monocytes into adipose tissues in obese mice. PSGL-1 is a candidate for a novel therapeutic target for prevention of obesity-related insulin resistance.

## ACKNOWLEDGMENTS

This study was supported in part by Grants-in-Aid for Scientific Research from the Ministry of Education, Science, Culture, Sports, and Technology of Japan.

No potential conflicts of interest relevant to this article were reported.

C.S. researched data, contributed to discussion, and wrote the manuscript. K.S. contributed to discussion and reviewed/edited the manuscript. D.H., M.S., S.N., S.M., R.K., A.T., J.W., and N.K. researched data. D.O. and H.M. reviewed/edited the manuscript. H.U.K. contributed to discussion.

We thank Dr. Kazuyuki Tobe and Dr. Shiho Fujisaka (Toyama University) for technical advice on FACS analysis.

## REFERENCES


1. Wellen KE, Hotamisligil GS. Inflammation, stress, and diabetes. J Clin Invest 2005;115:1111–1119
2. Weisberg SP, McCann D, Desai M, Rosenbaum M, Leibel RL, Ferrante AW Jr. Obesity is associated with macrophage accumulation in adipose tissue. J Clin Invest 2003;112:1796–1808
3. Xu H, Barnes GT, Yang Q, Tan G, Yang D, Chou CJ, Sole J, Nichols A, Ross JS, Tartaglia LA, Chen H. Chronic inflammation in fat plays a crucial role in the development of obesity-related insulin resistance. J Clin Invest 2003;112:1821–1830
4. Hotamisligil GS, Shargill NS, Spiegelman BM. Adipose expression of tumor necrosis factor-alpha: direct role in obesity-linked insulin resistance. Science 1993;259:87–91
5. Takahashi K, Mizuarai S, Araki H, Mashiko S, Ishihara A, Kanatani A, Itadani H, Kotani H. Adiposity elevates plasma MCP-1 levels leading to the increased CD11b-positive monocytes in mice. J Biol Chem 2003;278: 46654–46660
6. Kanda H, Tateya S, Tamori Y, Kotani K, Hiasa K, Kitazawa R, Kitazawa S, Miyachi H, Maeda S, Egashira K, Kasuga M. MCP-1 contributes to macrophage infiltration into adipose tissue, insulin resistance, and hepatic steatosis in obesity. J Clin Invest 2006;116:1494–1505
7. Weisberg SP, Hunter D, Huber R, Lemieux J, Slaymaker S, Vaddi K, Charo I, Leibel RL, Ferrante AW Jr. CCR2 modulates inflammatory and metabolic effects of high-fat feeding. J Clin Invest 2006;116:115–124
8. Kamei N, Tobe K, Suzuki R, Ohsugi M, Watanabe T, Kubota N, Ohtsuka-Kowatari N, Kumagai K, Sakamoto K, Kobayashi M, Yamauchi T, Ueki K, Oishi Y, Nishimura S, Manabe I, Hashimoto H, Ohnishi Y, Ogata H, Tokuyama K, Tsunoda M, Ide T, Murakami K, Nagai R, Kadowaki T. Overexpression of monocyte chemoattractant protein-1 in adipose tissues causes macrophage recruitment and insulin resistance. J Biol Chem 2006;281:26602–26614
9. Bevilacqua MP, Nelson RM. Selectins. J Clin Invest 1993;91:379–387
10. Hirata K, Shikata K, Matsuda M, Akiyama K, Sugimoto H, Kushiro M, Makino H. Increased expression of selectins in kidneys of patients with diabetic nephropathy. Diabetologia 1998;41:185–192
11. Sugimoto H, Shikata K, Hirata K, Akiyama K, Matsuda M, Kushiro M, Shikata Y, Miyatake N, Miyasaka M, Makino H. Increased expression of intercellular adhesion molecule-1 (ICAM-1) in diabetic rat glomeruli: glomerular hyperfiltration is a potential mechanism of ICAM-1 upregulation. Diabetes 1997;46:2075–2081
12. Okada S, Shikata K, Matsuda M, Ogawa D, Usui H, Kido Y, Nagase R, Wada J, Shikata Y, Makino H. Intercellular adhesion molecule-1-deficient mice are resistant against renal injury after induction of diabetes. Diabetes 2003;52:2586–2593
13. Chow FY, Nikolic-Paterson DJ, Ozols E, Atkins RC, Tesch GH. Intercellular adhesion molecule-1 deficiency is protective against nephropathy in type 2 diabetic db/db mice. J Am Soc Nephrol 2005;16:1711–1722
14. Leinonen E, Hurt-Camejo E, Wiklund O, Hulten LM, Hiukka A, Taskinen MR. Insulin resistance and adiposity correlate with acute-phase reaction and soluble cell adhesion molecules in type 2 diabetes. Atherosclerosis 2003;166:387–394
15. Targher G, Bonadonna RC, Alberiche M, Zenere MB, Muggeo M, Bonora E. Relation between soluble adhesion molecules and insulin sensitivity in type 2 diabetic individuals: role of adipose tissue. Diabetes Care 2001;24: 1961–1966
16. Straczkowski M, Lewczuk P, Dzienis-Straczkowska S, Kowalska I, Stepien A, Kinalska I. Elevated soluble intercellular adhesion molecule-1 levels in obesity: relationship to insulin resistance and tumor necrosis factor-alpha system activity. Metabolism 2002;51:75–78
17. Troseid M, Lappegard KT, Mollnes TE, Arnesen H, Seljeflot I. Changes in serum levels of E-selectin correlate to improved glycaemic control and reduced obesity in subjects with the metabolic syndrome. Scand J Clin Lab Invest 2005;65:283–290
18. Couillard C, Ruel G, Archer WR, Pomerleau S, Bergeron J, Couture P, Lamarche B, Bergeron N. Circulating levels of oxidative stress markers and endothelial adhesion molecules in men with abdominal obesity. J Clin Endocrinol Metab 2005;90:6454–6459
19. Xia L, Sperandio M, Yago T, McDaniel JM, Cummings RD, Pearson-White S, Ley K, McEver RP. P-selectin glycoprotein ligand-1-deficient mice have impaired leukocyte tethering to E-selectin under flow. J Clin Invest 2002;109:939–950
20. Yang J, Hirata T, Croce K, Merrill-Skoloff G, Tchernychev B, Williams E, Flaumenhaft R, Furie BC, Furie B. Targeted gene disruption demonstrates that P-selectin glycoprotein ligand 1 (PSGL-1) is required for P-selectin-mediated but not E-selectin-mediated neutrophil rolling and migration. J Exp Med 1999;190:1769–1782
21. Dennis G Jr, Sherman BT, Hosack DA, Yang J, Gao W, Lane HC, Lempicki RA. DAVID: Database for Annotation, Visualization, and Integrated Discovery. Genome Biol 2003;4:P3
22. Hirata T, Merrill-Skoloff G, Aab M, Yang J, Furie BC, Furie B. P-Selectin glycoprotein ligand 1 (PSGL-1) is a physiological ligand for E-selectin in mediating T helper 1 lymphocyte migration. J Exp Med 2000;192:1669–1676
23. Joost HG, Schurmann A. Subcellular fractionation of adipocytes and 3T3–L1 cells. Methods Mol Biol 2001;155:77–82
24. Eguchi J, Wada J, Hida K, Zhang H, Matsuoka T, Baba M, Hashimoto I, Shikata K, Ogawa N, Makino H. Identification of adipocyte adhesion molecule (ACAM), a novel CTX gene family, implicated in adipocyte maturation and development of obesity. Biochem J 2005;387:343–353
25. Ogawa D, Shikata K, Honke K, Sato S, Matsuda M, Nagase R, Tone A, Okada S, Usui H, Wada J, Miyasaka M, Kawashima H, Suzuki Y, Suzuki T, Taniguchi N, Hirahara Y, Tadano-Aritomi K, Ishizuka I, Tedder TF, Makino H. Cerebroside sulfotransferase deficiency ameliorates L-selectin-dependent monocyte infiltration in the kidney after ureteral obstruction. J Biol Chem 2004;279:2085–2090
26. Folch J, Lees M, Sloane Stanley GH. A simple method for the isolation and purification of total lipids from animal tissues. J Biol Chem 1957;226:497–509
27. Hicks AE, Nolan SL, Ridger VC, Hellewell PG, Norman KE. Recombinant P-selectin glycoprotein ligand-1 directly inhibits leukocyte rolling by all 3 selectins in vivo: complete inhibition of rolling is not required for anti-inflammatory effect. Blood 2003;101:3249–3256
28. Norman KE, Katopodis AG, Thoma G, Kolbinger F, Hicks AE, Cotter MJ, Pockley AG, Hellewell PG. P-selectin glycoprotein ligand-1 supports rolling on E- and P-selectin in vivo. Blood 2000;96:3585–3591
29. Yang J, Furie BC, Furie B. The biology of P-selectin glycoprotein ligand-1: its role as a selectin counterreceptor in leukocyte-endothelial and leukocyte-platelet interaction. Thromb Haemost 1999;81:1–7
30. Sako D, Chang XJ, Barone KM, Vachino G, White HM, Shaw G, Veldman GM, Bean KM, Ahern TJ, Furie B, et al. Expression cloning of a functional glycoprotein ligand for P-selectin. Cell 1993;75:1179–1186
31. Yang J, Galipeau J, Kozak CA, Furie BC, Furie B. Mouse P-selectin glycoprotein ligand-1: molecular cloning, chromosomal localization, and expression of a functional P-selectin receptor. Blood 1996;87:4176–4186
32. McEver RP, Cummings RD. Role of PSGL-1 binding to selectins in leukocyte recruitment. J Clin Invest 1997;100:S97–S103
33. Dong ZM, Gutierrez-Ramos JC, Coxon A, Mayadas TN, Wagner DD. A new class of obesity genes encodes leukocyte adhesion receptors. Proc Natl Acad Sci U S A 1997;94:7526–7530
34. Robker RL, Collins RG, Beaudet AL, Mersmann HJ, Smith CW. Leukocyte migration in adipose tissue of mice null for ICAM-1 and Mac-1 adhesion receptors. Obes Res 2004;12:936–940
35. Lumeng CN, Bodzin JL, Saltiel AR. Obesity induces a phenotypic switch in adipose tissue macrophage polarization. J Clin Invest 2007;117:175–184
36. Amersi F, Farmer DG, Shaw GD, Kato H, Coito AJ, Kaldas F, Zhao D, Lassman CR, Melinek J, Ma J, Volk HD, Kupiec-Weglinski JW, Busuttil RW. P-selectin glycoprotein ligand-1 (rPSGL-Ig)-mediated blockade of CD62 selectin molecules protects rat steatotic liver grafts from ischemia/reperfusion injury. Am J Transplant 2002;2:600–608
37. Inoue T, Tsuzuki Y, Matsuzaki K, Matsunaga H, Miyazaki J, Hokari R, Okada Y, Kawaguchi A, Nagao S, Itoh K, Matsumoto S, Miura S. Blockade of PSGL-1 attenuates CD14+ monocytic cell recruitment in intestinal mucosa and ameliorates ileitis in SAMP1/Yit mice. J Leukoc Biol 2005;77: 287–295
38. Rivera-Nieves J, Burcin TL, Olson TS, Morris MA, McDuffie M, Cominelli F, Ley K. Critical role of endothelial P-selectin glycoprotein ligand 1 in chronic murine ileitis. J Exp Med 2006;203:907–917
39. Hosoda K, Masuzaki H, Ogawa Y, Miyawaki T, Hiraoka J, Hanaoka I, Yasuno A, Nomura T, Fujisawa Y, Yoshimasa Y, Nishi S, Yamori Y, Nakao K. Development of radioimmunoassay for human leptin. Biochem Biophys Res Commun 1996;221:234–239